2019 12th Asian Control Conference (ASCC)
Kitakyusyu International Conference Center
Japan, June 9-12, 2019

Investigation of lateral stiffness and damping in levitation system with opposite electromagnets*

A. K. Piłat[1], *Member, IEEE*, B. Sikora[2], J. Źrebiec[3]

***Abstract*— This paper contains research on magnetic levitation system with two electromagnetic actuators in E shape configuration, located anti-parallel. The document presents influence of the coil current in the operating point on the lateral stiffness and damping of the levitating object, under the external static and dynamic load. Numerical model and experimental research, validated with support of image processing, are presented. The lateral displacement is identified.**

I. INTRODUCTION

This research was motivated by the PD control operating in differential mode realised for magnetic levitation system with 2 electromagnets (MLS2EM) [1]. Moreover, the plenary talk given by Prof. Takeshi Mizuno from Saitama University, Japan, during 16^{th} International Symposium on Magnetic Bearings (ISMB16) described possibility of lateral vibration control by switching stiffness. Active magnetic levitation systems allows to counteract the gravitational force. Typically, solution with a single electromagnetic actuator, which may be supported by a permanent magnet, is used [2]. Application of two electromagnets, placed opposite each other [3], allows to conduct research on stabilizing regulators [4], [1], fuzzy logic controllers [5], up to model predictive control [6]. By using two actuators, a common configuration of a single axis active magnetic bearing may be applied. Its mathematical model and control methods are widely known [4], [7]. The finite element method (FEM) design approach may provide model, which is similar to the experimental one, and thus useful in the virtual prototyping [8]. However, effective control of a levitated rotor demands a multidimensional regulator. Static and dynamic regulator configuration, which is embedded into the hardware layer of an industrial programmable analog controller (PAC), is presented in [8]. Research on state observation of the single axis magnetic bearing with additional axial load, is conducted [9]. Extended a magnetic levitation system by an additional electromagnet leads to stability enhancement with 2-degrees of freedom (DOF) proportional-integral-derrivative (PID) controller [10].

*Research supported by AGH University of Science and Technology, Krakow, Poland

[1]A. K. Piłat is with the AGH University of Science and Technology, Department of Control Science and Robotics, Mickiewicza 30, 30-059 Kraków, Poland (phone: +48 12 6341568; fax: +48 12 6341568; e-mail: ap@agh.edu.pl)

[2]B. Sikora is a Ph.D. student at AGH University of Science and Technology, Department of Control Science and Robotics, Mickiewicza 30, 30-059 Kraków, Poland bsikora@agh.edu.pl

[3]J. Źrebiec is a Ph.D. student at AGH University of Science and Technology, Department of Control Science and Robotics, Mickiewicza 30, 30-059 Kraków, Poland jzrebiec@agh.edu.pl

This paper describes the implementation of the configurable load, which acts on the levitating sphere in the axis perpendicular to its axial motion. The scientific novelty is included in the extended analysis of the MLS2EM lateral stiffness and damping, by investigating lateral motion of the sphere, involving the FEM, image processing and experimental procedures. Following problems are discussed:

1) Does a control in a single axis, with both electromagnets in E configuration, located axially and anti-parallel, allow to minimize a motion in a perpendicular axis?
2) What is the distribution of the electromagnetic force components, for a variable position of the sphere, in the levitating space?
3) How do the dynamic properties of a closed-loop system change, when increasing a control of the electromagnetic actuators?
4) How does a control of the actuator influence on the lateral static and dynamic load?

II. ANALYTICAL MODEL

The laboratory test-rig MLS2EM consists of two electromagnets operating in differential mode. Widespread configuration of the electromagnetic actuator in the system composes of the core in a "E" shape of a horseshoe and two windings located on both pole pieces.

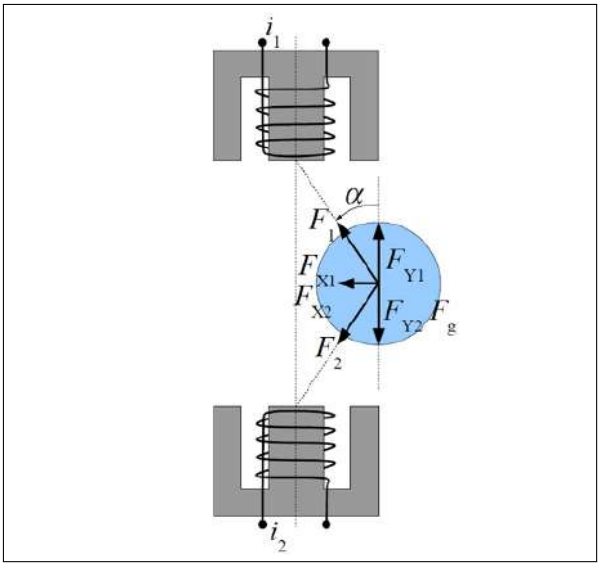

Fig. 1. Distribution of the electromagnetic force components, when the sphere is displaced horizontally from the center - steady-state levitation point.

Mathematical model of the single axis magnetic levitation system [4] with hardware coil current regulators (Fig. 1) may be expressed by the following set of equations:

$$\begin{cases} \dot{x}_1 = x_2 \\ \dot{x}_2 = \frac{1}{2 \cdot m_s} \left(\frac{dL(x_1)}{dx_1} \cdot x_3^2 - \frac{dL(x_t - x_1)}{d(x_t - x_1)} \cdot x_4^2 + F_g \right) \\ \dot{x}_3 = \frac{1}{T_3} \cdot (k_3(u_1 + u_{c3}) - x_3) \\ \dot{x}_4 = \frac{1}{T_4} \cdot (k_4(u_2 + u_{c4}) - x_4) \end{cases} \quad (1)$$

where state variables x_1,x_2,x_3,x_4 are respectively position and velocity of the sphere, current of the top and bottom electromagnet. Control applied to the actuator units stands as u_1 and u_2.

TABLE I
PARAMETERS OF THE REAL MLS2EM SYSTEM

Parameter	Symbol	Value
mass of the sphere	m_s	38.7$[g]$
mass of the static load	m_l	8.5$[g]$
total air gap	x_t	21$[mm]$
external sphere radius	R_e	29.5$[mm]$
number of coil turns	N_T	640
resistance of the coil	R	4.3$[\Omega]$
time constant of the electromagnet	T_3, T_4	10$[ms]$
gain coefficient	k_3, k_4	0.64$[A/V]$
constant coil voltage	u_{c3}, u_{c4}	0.045$[V]$
constant coil current	i_{03}, i_{04}	0.23$[A]$
the coil inductance at x_1=0	L_0	40.8$[mH]$
derivative of the coil inductance	$\frac{dL(x_1)}{dx_1} = a \cdot e^{bx_1}$	a= 6.996 b=-171.5

Table I shows key parameters of the real MLS2EM system, which were identified experimentally. Figure 2 presents derivative of the coil inductance over the axial position of the sphere.

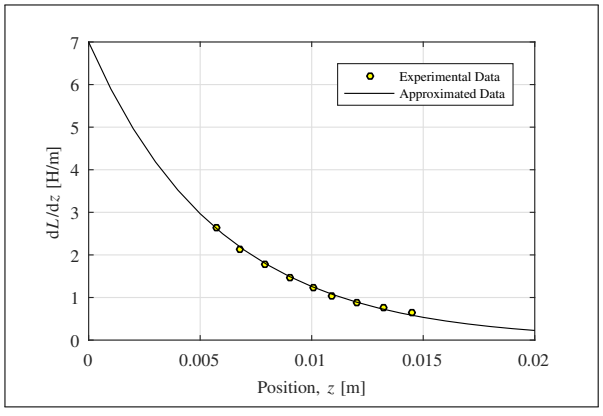

Fig. 2. Derivative of the inductance over the sphere's axial position.

III. NUMERICAL MODEL

The three-dimensional (3D) numerical model of the MLS2EM system was developed in COMSOL Multipysics

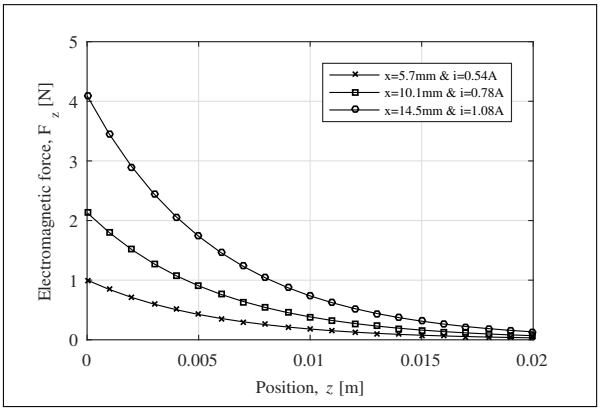

Fig. 3. The electromagnetic force characteristic $F(x_0, i_0)$ obtained from experiments of PD stabilization, close to the MLS2EM operational point.

(Fig. 4) to calculate the electromagnetic force components with respect to the levitating object displacement and applied coil current. A single set of the calculations is presented in Figs. 5 and 6. Note, that the axial force depends on the object displacement, and therefore the control of dynamical properties in lateral direction is possible. An initial comparison between numerical and experimental set-up was done to check the convergence (see Fig. 7). Extra identification and modeling research should be done to achieve a full convergence.

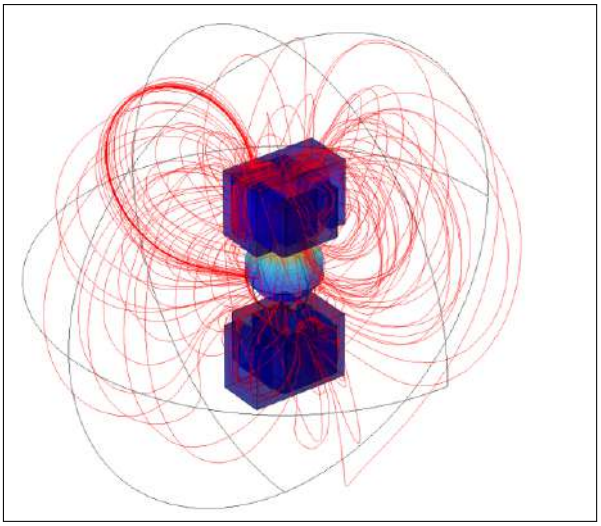

Fig. 4. Developed 3d numerical model of the MLS2EM.

IV. TEST-RIG

The laboratory test-rig MLS2EM [3] was modified, to fulfill planned research requirements, as follows (see Fig. 8):

- a power amplifier with a current controller (with an internal hardware feedback loop, in order to maintain the current set value) was applied,
- static load in the form of a mass hanging on a thread,
- a side electromagnet was used to excitate a lateral motion of the levitated sphere,
- a camera was used for additional observation of the sphere motion.

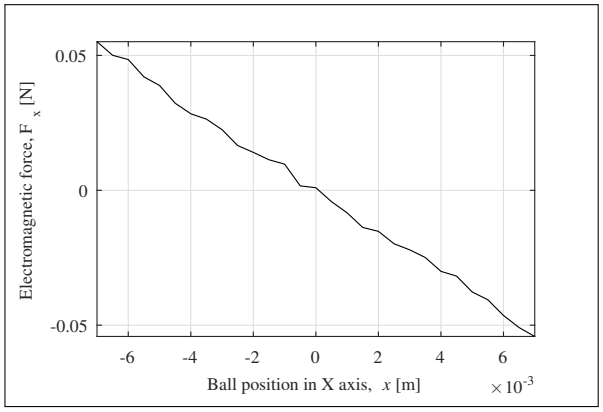

Fig. 5. The electromagnetic force $F_x(x)$ from the numerical model.

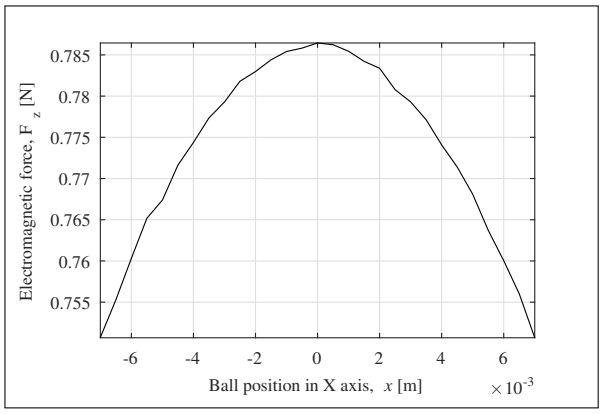

Fig. 6. The electromagnetic force $F_z(x)$ from the numerical model.

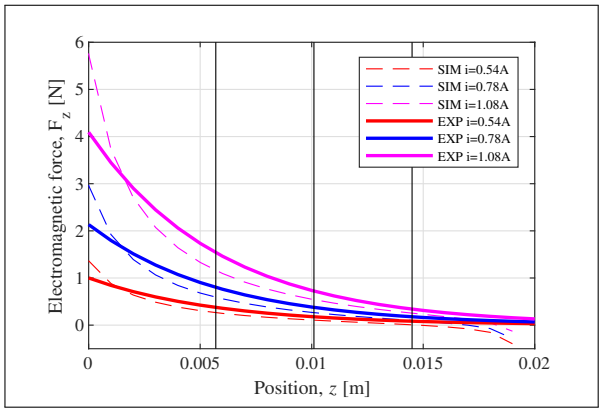

Fig. 7. Comparison between the electromagnetic force, from the identification and the numerical model, for a few selected MLS2EM operational points.

V. METHOD OF SPHERE MOTION DETECTION

In order to determine the horizontal displacement of the sphere, the additional sensor must be utilized. The Logitech C920 camera was used, as a tool for global observation of the sphere's location. This camera does not allow to close the real-time video feedback in a control loop. Also, limited data acquisition and transfer to 30 frames per second, at resolution of 1080x720, narrows the possible observation range of the sphere's motion. Therefore, the recorded video material is analyzed off-line, in order to reconstruct the motion of the

Fig. 8. Upgraded MLS2EM test-rig for research purposes.

sphere in the levitating space. The red-green-blue (RGB) image is transformed into the monochrome image and then binarized. The sphere surface is covered, to obtain the full circle shape. Then, the center of mass is determined, which is the representation of its center.

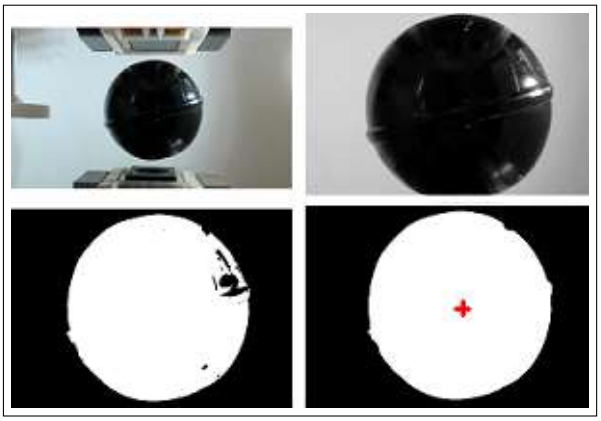

Fig. 9. Operation example of the sphere's displacement detection, based on recorded video file.

An image was recorded and stored with a frequency of 30 fps, irrespectively from the experiment conducted in real time, with the sampling frequency of 1kHz ($T_0 = 1ms$) under supervision of Simulink Real-Time desktop running in MATLAB/Simulink, at Windows 7. After registration of the video material and experimental data, the content of files was processed, in order to obtain particular sphere's displacements. The waveforms were synchronized, based on the alignment of the sphere's displacement in the vertical direction (axial alignment of electromagnets). The stabilizing

controller was realized in a differential mode to keep the sphere levitating in the center between electromagnets.

$$u(k) = e(k)(K_p + K_d {T_0}^{-1}) - e(k-1)K_d {T_0}^{-1} \quad (2)$$

$$u_1(k) = u_{10} + u(k) \quad (3)$$

$$u_2(k) = u_{20} - u(k) \quad (4)$$

where: $e(k) = x_{10}(k) - w$, u_{10}, u_{20} - is a steady state control applied to upper and lower electromagnet respectively, T_0 is a sampling period ($1ms$), K_p, K_d are proportional and derivative parameters of the stabilizing controller. Choosing the values of K_p, K_d, u_{10}, and u_{20} the dynamical properties of the levitation system can be set-up. Due to the current feedback applied in the hardware, the control signal is proportional to the coil current and therefore its time diagrams will be omitted.

VI. ANALYSIS AND ESTIMATION OF LATERAL DISPLACEMENT

Based on image processing, a waveform, which represents vertical and horizontal displacement of the sphere, is obtained. From the control theory point of view, according to the dynamics of the active magnetic levitation system, it is particularly interesting to know the dynamic properties in the horizontal axis, when controlling the vertical axis motion of the sphere. Low image acquisition frequency affects strongly the quality of the reconstructed displacement signal. It is assumed that the dynamical motion of the levitating sphere in a horizontal axis is described by the second order linear system. Therefore, the lateral oscillatory motion can be formulated in a form of equation (5). In order to more accurately determine the frequency of horizontal vibrations of the sphere and the damping coefficient, the experimental data was approximated by the (5).

$$x(t) = A \cdot e^{-\delta \cdot t} \cdot sin(\omega t + \phi) \quad (5)$$

where A, δ, ω and ϕ denote, respectively, amplitude of vibration, exponential coefficient providing vibration attenuation, signal frequency and its phase shift. Approximation procedure based on (5) and scaled with resolution values from the Logitech C920 (resolution in X and Y axis is 107.69 [μm] and 109.80 [μm]) were used to identify the lateral motion of the levitating object.

VII. INVESTIGATION OF LATERAL MOTION UNDER STATIC LOAD

Aim of this experiment was to levitate the sphere with the attached mass (see Fig. 10) and increasing the control of the upper and lower electromagnet. Based on the control change analysis and as a consequence of the linear steady-state current change, one can observe the effect of the electromagnetic force change affecting the levitating sphere. The rising electromagnetic force will cause attraction of the sphere towards the axis of electromagnets. When lowering the force value, the sphere moves toward the static load. This experiment allows to scale the electromagnetic force on the basis of the external load (see Figs. 11 ÷ 13). Please note, that due to the stabilization given by the controller, the sphere is kept close to the desired position.

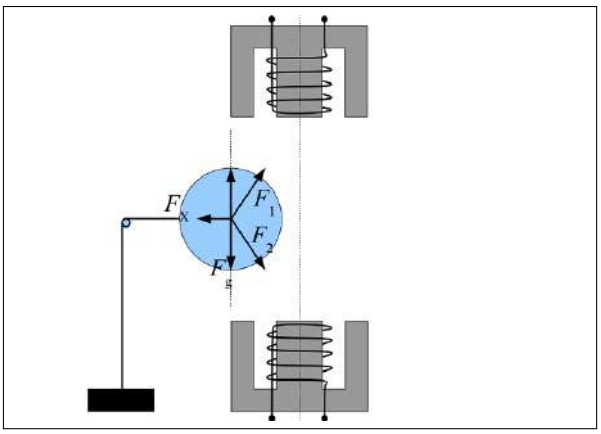

Fig. 10. Levitation scenario under the static load - the mass hanging on the thread.

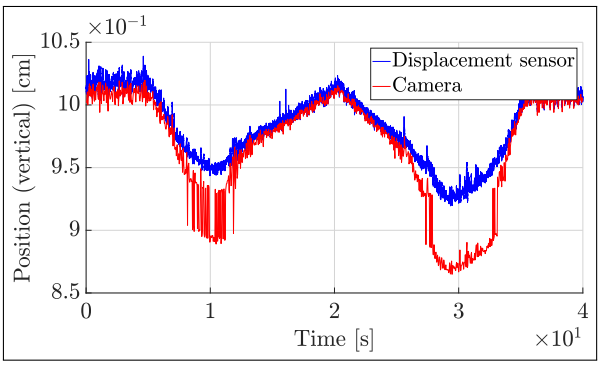

Fig. 11. Displacement in vertical axis of the levitating sphere

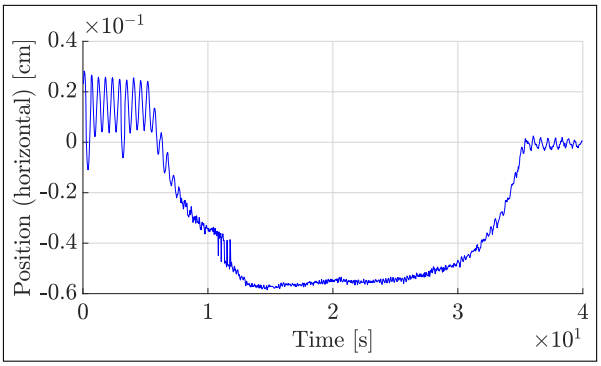

Fig. 12. Displacement in horizontal axis of the levitating sphere

VIII. INVESTIGATION OF LATERAL MOTION UNDER DYNAMIC LOAD

Aim of this experiment was to levitate the sphere, turn-on and turn off the external excitation in horizontal axis, by using an electromagnet (see Fig. 14).

With this non-contact method, the sphere will be pulled out from the center position. The angle α (see Fig. 1)

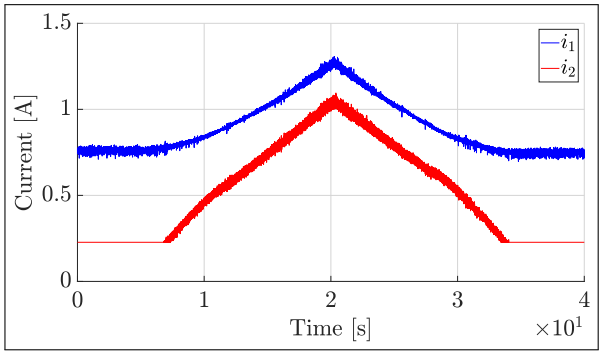

Fig. 13. Coil current in the static load experiment.

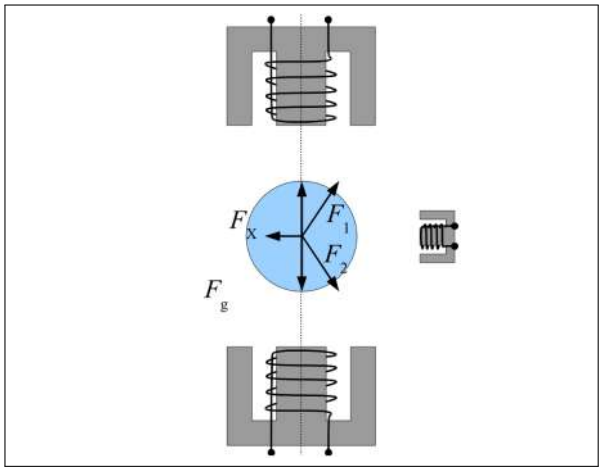

Fig. 14. Levitation scenario under the dynamic load - the horizontally located electromagnet, which generates variable lateral force.

appears, and the forces F_1 and F_2 have horizontal and vertical components. When the external force is realized, the sphere returns to the central position (see Figs. 15 ÷ 17).

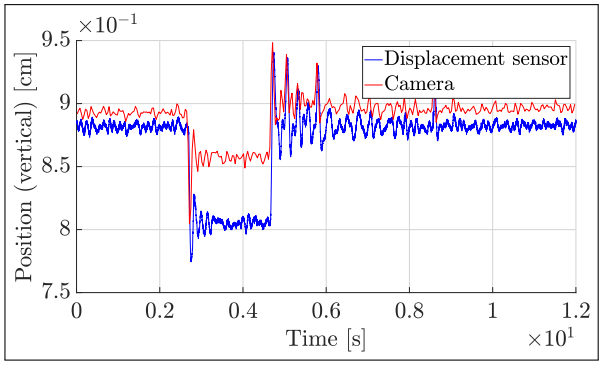

Fig. 15. Displacement in vertical axis of the levitating sphere - test 1

The dynamics of motion depends on the stabilizing controller and its parameters. Two experimental results were compared for the modified steady state control. The parameters of the controller were set as follows: $K_p = 250$, $K_d = 2$, while steady state current was applied as $i_{10} = 0.76A$ and $i_{20} = 0.23A$ for scenario A (see Fig. 18), and $i_{10} = 1.44A$ and $i_{20} = 1.18A$ for scenario B (see Fig. 19). The horizontal displacements were registered, analyzed, and fitted with the proposed analytical response. The coefficients of the equation

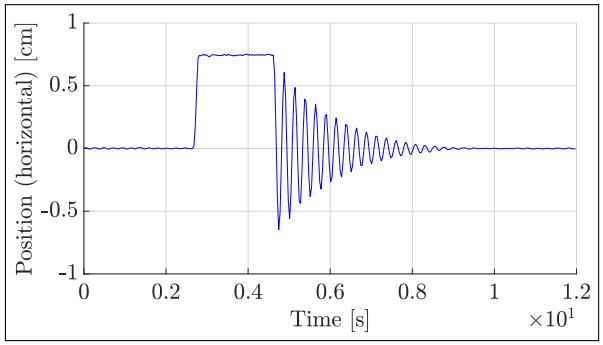

Fig. 16. Displacement in horizontal axis of the levitating sphere - test 1

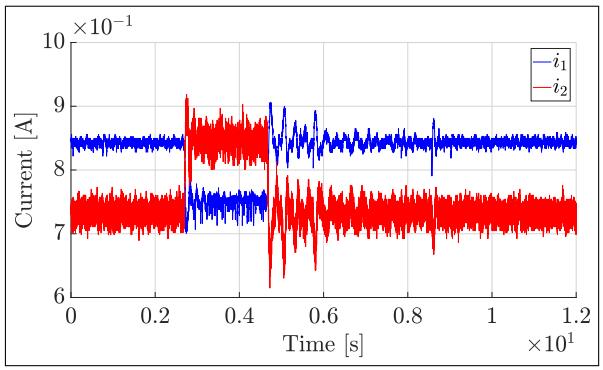

Fig. 17. Coil current in the dynamic load mode - test 1

(5) are listed in Table II (for scenario A and B). Note, that the stretching action of electromagnetic forces results in system dynamics.

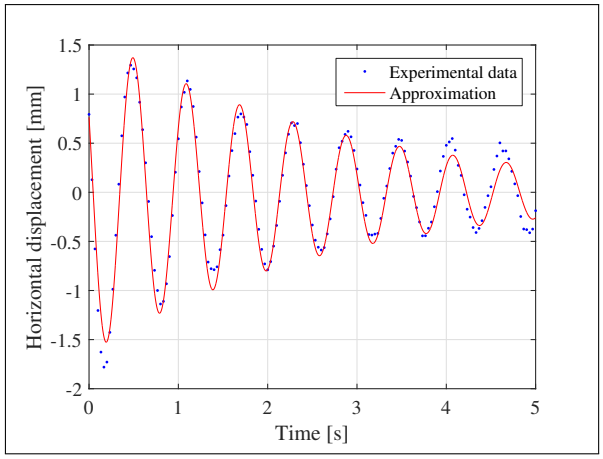

Fig. 18. Horizontal displacement in scenario A

TABLE II
RESULTS OF EXPERIMENTAL DATA ANALYSIS

Config	A	δ	ω	ϕ
A	1.6364	0.3603	10.5241	2.6562
B	-0.8946	0.8788	41.4604	-0.0323

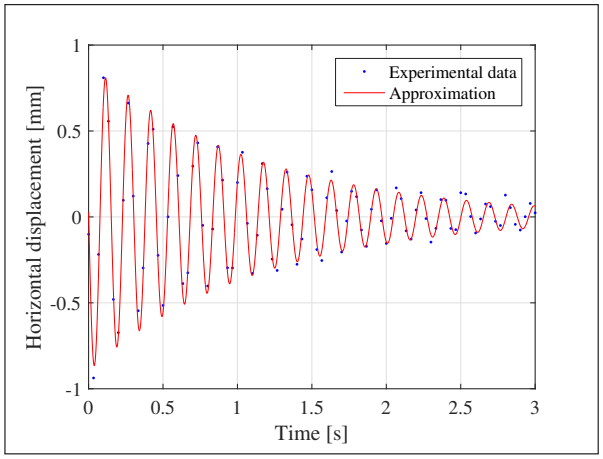

Fig. 19. Horizontal displacement in scenario B

IX. GENERALIZATION

On the basis of conducted research, we propose the generalization (6) of the Active Magnetic Levitation/Bearing system to the 3D model, when the model consists of a single electromagnet or two electromagnets, located opposite to each other, with a controlled axial motion of a levitating object.

$$\begin{cases} M\ddot{x} = F(x,i) + G \\ \dot{i} = f_i(x,i,u) \end{cases} \tag{6}$$

where: x stands a displacement vector, i is a coil current vector, u is a control vector, f_i is a function, that describes dynamics of the electromagnetic actuators, M is a mass matrix, $F(\cdot)$ is a force matrix, and G is a gravity matrix.

X. CONCLUSIONS

The conducted research confirmed, that the dynamical properties of lateral motion can be configured by the stretching control. The numerical model informed about all electromagnetic force components, with respect to the object displacement. This research demonstrated, that it is possible to simplify and minimize a construction of an active magnetic levitation and an active magnetic bearing to two electromagnets, if stretching forces are sufficient to stabilize the levitating object under external disturbances. The experimental results informed about non-linear lateral motion of the levitating sphere. The future research will be focused on the detailed analysis of motion nonlinearities and precise calculation of forces components with respect to the controller configurations. It is requested to apply high speed camera or other method, in order to precisely identify the levitating object displacement.

REFERENCES

[1] A. Pilat. "Testing Performance and Reliability of Magnetic Suspension Controllers". In: *IFAC Proceedings Volumes* 42.13 (2009). 14th IFAC Conference on Methods and Models in Automation and Robotics, pp. 164–167.

[2] T. Mizuno. "Vibration Isolation System using zero-power magnetic suspension". In: *IFAC Proceedings Volumes* 35.1 (2002). 15th IFAC World Congress, pp. 25–30. ISSN: 1474-6670.

[3] InTeCo. *Active magnetic levitation system MLS1EM, MLS2EM - User's Guide*. INTECO, Krakow, Poland, 2005. URL: www.inteco.com.pl.

[4] A. Pilat. *Active Magnetic Levitation Systems*. AGH University of Science and Technology, 2002, pp. 1–100.

[5] C. Bojan-Dragos et al. "Takagi-Sugeno fuzzy controller for a magnetic levitation system laboratory equipment". In: *2010 International Joint Conference on Computational Cybernetics and Technical Informatics*. May 2010, pp. 55–60.

[6] C. Bojan-Dragos et al. "Model predictive control solution for magnetic levitation systems". In: *2015 20th International Conference on Methods and Models in Automation and Robotics*. Aug. 2015, pp. 139–144.

[7] A. Pilat. *Active magnetic levitation systems*. AGH University of Science and Technology, 2013.

[8] A. Pilat. "Modeling, Simulation and Control of Dual Electromagnet Active Magnetic Levitation". In: *Proceedings of the 2012 COMSOL Conference*. 2012.

[9] A. Bonfitto et al. "Offset-Free Model Predictive Control for Active Magnetic Bearing Systems". In: *Actuators* 7.3 (2018).

[10] H. Huang, H. Du, and W. Li. "Stability enhancement of magnetic levitation ball system with two controlled electomagnets". In: *2015 Australasian Universities Power Engineering Conference (AUPEC)*. Sept. 2015, pp. 1–6.